Dual-wavelength operation of continuous-wave and mode-locked erbium-doped fiber lasers

O. Pottiez*[a], A. Martinez-Rios[a], D. Monzon-Hernandez[a], B. Ibarra-Escamilla[b], E.A. Kuzin[b], J.C. Hernandez-Garcia[a]

[a]Centro de Investigaciones en Óptica, 115 Loma del Bosque, León, Gto., Mexico 37150;
[b]Instituto Nacional de Astrofísica, Óptica y Electrónica, 1 L.E. Erro, Puebla, Pue., Mexico 72000

ABSTRACT

We study numerically and experimentally multiple-wavelength operation of an erbium-doped figure-eight fiber laser including a multiple-bandpass optical filter formed by two concatenated fiber tapers. Both continuous-wave and pulsed operations are considered. In the continuous-wave regime, stable long-term operation at multiple closely spaced wavelengths is only obtained if fine adjustments of the cavity losses are performed. Under these conditions, simultaneous lasing at up to four wavelengths separated by *1.5 nm* was observed experimentally. Tunable single-wavelength operation over more than *20 nm* is also observed in the continuous-wave regime. In the passive mode locking regime, numerical simulations indicate that mechanisms involving the filter losses and the nonlinear transmission characteristic of the NOLM contribute in principle to stabilize dual-wavelength operation, allowing less demanding cavity loss adjustments. In this regime, the problem of synchronization between the pulse trains generated at each wavelength adds an additional dimension to the problem. In presence of cavity dispersion, the pulses at each wavelength tend to be asynchronous if the wavelength separation is large, however they can be synchronous in the case of closely spaced wavelengths, if cross-phase modulation is able to compensate for the dispersion-induced walkoff. Experimentally, fundamental and 2nd-order harmonic mode locking was observed, characterized by the generation of noise-like pulses. Finally, a regime of multi-wavelength passive Q-switching was also observed. We believe that this work will be helpful to guide the design of multiple-wavelength fiber laser sources, which are attractive for a wide range of applications including Wavelength Division Multiplexing transmissions, signal processing and sensing.

Keywords: Nonlinear Optical Loop Mirror, Wavelength filtering devices, Mode-locked fiber lasers, Erbium fiber lasers

1. INTRODUCTION

Fiber lasers are versatile low-cost sources that are attractive for many applications. In continuous-wave mode, tunable and multiwavelength laser sources are required for wavelength division multiplexing (WDM), fiber sensors and optical instrument calibration, for example. On the other hand, thanks to techniques like passive Q-switching and passive mode locking, fiber lasers are able to generate short and ultrashort pulses, respectively, whose peak power is much higher than the continuous-wave power, allowing in particular the use of these sources for studying and exploiting nonlinear effects in fibers, a framework in which supercontinuum generation deserves a particular mention. Although they are attractive for applications, passive pulsed multiwavelength fiber laser sources received relatively little interest in the literature.[1-8]

Passively mode-locked figure-eight fiber lasers are simple, compact and low-cost sources of ultrashort pulses that are attractive for a wide range of applications.[9] In such devices, the role of saturable absorber is played by a nonlinear optical loop mirror (NOLM),[10] or alternatively by a nonlinear amplifying loop mirror (NALM),[11] which is inserted in a ring structure. The nonlinear characteristic of a NOLM or NALM is due to the Kerr-induced nonlinear phase difference between the beams that counter-propagate in the loop, and takes the form of a smooth, sine-like function of input power. An inconvenient of conventional NOLMs however is the limited flexibility of the switching characteristic.

*pottiez@cio.mx; phone +52 477 4414200 ext 288; fax +52 477 4414209; cio.com.mx

Whereas in conventional NOLM schemes, switching relies on a power imbalance between the beams that counter-propagate in the loop, an alternative design was proposed,[12] based on polarization asymmetry. As a 50/50 coupler is used, the device is power-symmetric, and polarization symmetry is broken by the use of a quarter-wave retarder (QWR) in the loop. Nonlinear polarization rotation (NPR) replaces self-phase modulation as the key nonlinear effect that provides switching. The fiber is twisted to eliminate random polarization evolution along the loop, and to increase the device robustness against environmental perturbations. Among the device advantages is the flexibility of its nonlinear switching characteristic, which can be adjusted through the orientation of the QWR or the choice of input polarization. Stable generation of sub-ps pulses by a figure-eight laser including such a NOLM architecture was demonstrated experimentally.[13] It was also shown that a precise adjustment of the NOLM low-power transmission through the QWR orientation allows self-starting mode locking operation.[14] By inserting an adjustable bandpass filter in the laser cavity, wavelength-tunable ps pulse generation was demonstrated.[15] Finally, by controlling the angle of linear input polarization, the switching power can be adjusted continuously between a minimum value and infinity, without affecting the low-power transmission.[16,17]

In this paper, we propose and study experimentally a figure-eight laser scheme based on a polarization-imbalanced NOLM whose switching characteristic is controlled through QWR angle and linear input polarization orientation. The device includes a periodic optical filter formed by two fiber tapers in series. Several modes of operation are evidenced in both continuous-wave and pulsed regimes. A numerical study is also performed that is useful for interpreting the experimental results in the pulsed regimes.

2. EXPERIMENTAL SETUP

The experimental setup is presented in Fig. 1. The figure-eight laser is formed by a ring laser cavity (left side of the figure) in which a NOLM is inserted (right part). The ring cavity includes a 4-m long Erbium-doped fiber (EDF) with *1000 ppm* erbium concentration, which is pumped by a 980-nm laser diode through a WDM coupler. The maximum pump power that can be coupled into the fiber is estimated to be *~300 mW*. A polarizer is inserted in the loop, as well as a polarization controller (PC) consisting of two retarder plates, which is used to maximize the power transmission through the polarizer. An optical isolator ensures unidirectional laser operation. A half-wave retarder (HWR) plate controls the angle ψ of linear polarization at the NOLM input. Two output couplers (*10%* output coupling) provide the laser output ports. The ring also includes an optical filter, which consists of two concatenated fused fiber tapers (Fig. 2(a)). The filter was fabricated in a Nufern 980HP fiber using a Vytran glass processor. The principle of the device is that of a Mach-Zehnder interferometer: at the first taper the fundamental core mode partially couples to cladding modes, and a fraction of the light guided in the cladding modes couples back to the core mode at the second taper.[18] The transmission spectrum of the filter is thus a periodic pattern resulting from the interference between core and cladding modes of the fiber (Fig. 2(b)). For the device dimensions used in this work and given in Fig. 2(a), the interference pattern presents a period of *1.65 nm*, a modulation depth of *~6 dB* and an insertion loss of *~0.5 dB*. It has to be noted that no bending was applied to the filter.

The NOLM is formed by a 51/49 coupler, whose output ports were fusion-spliced with a 100-m loop of low-birefringence, highly twisted Corning SMF-28 fiber. A QWR is inserted in the loop to transform the polarization of the counter-clockwise beam from linear to elliptic, the value of ellipticity depending on the relative angle α between the QWR and the polarizer. A twist rate of *5 turns/m* is imposed to the fiber loop, which is used to eliminate residual fiber birefringence so that the fiber behaves like an ideal isotropic fiber.[19] The fiber loop has an anomalous dispersion of *~17 ps/nm/km* and a nonlinear coefficient $\gamma = 1.5\ W^{-1}km^{-1}$ for linearly polarized light ($\beta = 2/3\gamma = 1\ W^{-1}km^{-1}$ for circular polarization). With these parameters, the minimum continuous-wave switching power of the NOLM is $P_\pi = 4\pi/\beta L \approx 125\ W$.[16] The operation of the NOLM is based on NPR, and allows great flexibility of the device transmission characteristic, which can be adjusted through the orientation of the QWR and of input polarization.
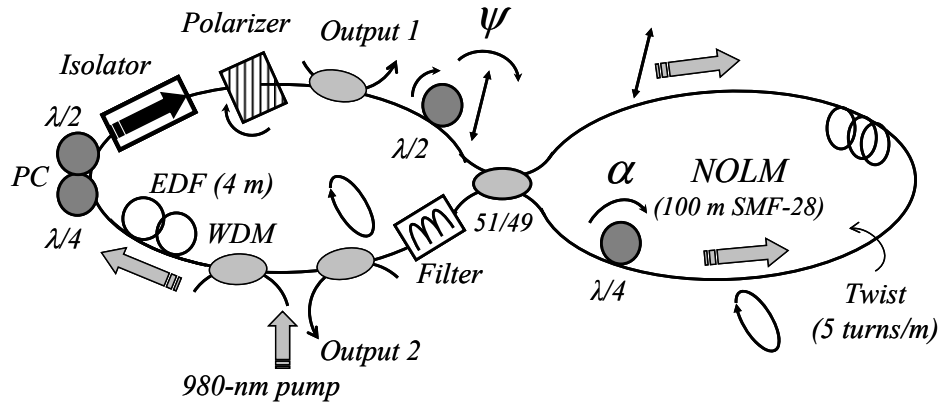
Figure 1. Experimental setup.

The QWR allows the adjustment of the NOLM low-power transmission, and also allows operating the NOLM as either saturable absorber or intensity limiter.[16] Moreover, in the saturable absorber mode, adjusting the NOLM low-power transmission is of key importance for mode locking operation, and to allow self starting.[14] On the other hand, when input polarization is linear, the adjustment of the orientation of input polarization allows adjusting the NOLM switching power. Let us assume for example that the QWR angle is adjusted for zero low-power transmission. Then, for linear input polarization forming an angle ψ with respect to the QWR axes, the NOLM transmission writes as $T = 0.5 - 0.5cos(\pi P_{in}/P_{\pi\psi})$, where P_{in} is the NOLM input power and $P_{\pi\psi} = P_{\pi}/sin(2\psi)$ is the switching power, which can be adjusted between P_{π} and infinity by adjusting the angle ψ. This mode of operation of the NOLM under linear input polarization was previously demonstrated theoretically[16] and experimentally.[17] Although these results are valid strictly speaking in the continuous-wave approximation only (case of large, ns pulses), they still apply qualitatively when ultrashort pulses are considered.[20] It has also to be noted that the same behavior is found even if the QWR angle departs from zero low-power transmission. Hence, QWR and input polarization adjustments allow a large flexibility of the NOLM switching characteristic, which in turn is responsible for the diversity of regimes observed experimentally.
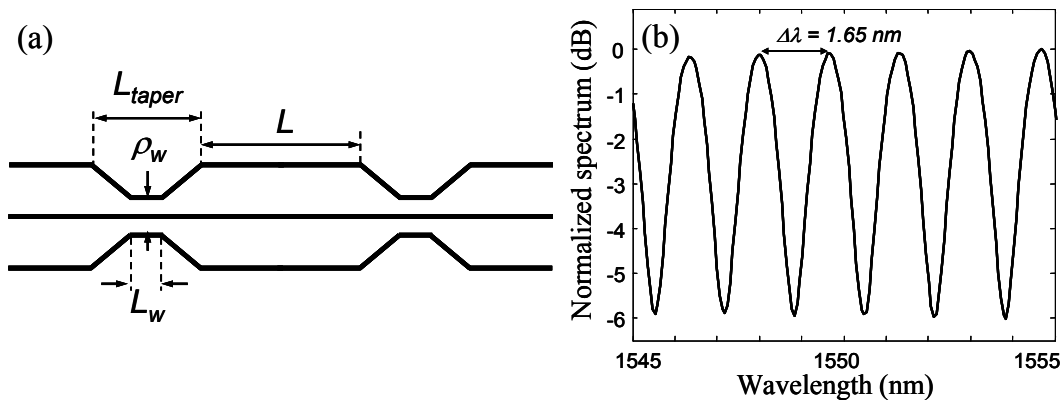
Figure 2. Optical filter formed by two identical fiber tapers in series: (a) schematic design and (b) transmission spectrum in the *1550 nm* region. Device parameters are: tapers separation $L = 25$ cm, total tapers length $L_{taper} = 5$ mm, waist diameter $\rho_w = 65$ μm and waist length $L_w = 1$ mm.

3. EXPERIMENTAL RESULTS

When the pump power is set to its maximal value, for most positions of the wave retarders, continuous-wave operation is obtained in the *1550 nm* region. As expected, the highest output power is observed at output 1, where it reaches up to ~*4 mW*. Adjustments of the retarder plates allows tuning single-wavelength laser oscillation over more than *20 nm*, between *1546 nm* and *1568 nm*, by steps of *1.65 nm*, corresponding to the filter spectral period (Fig. 3(a)). Single-wavelength

operation in the *1530 nm* region was also observed. In contrast, lasing in the *1540 nm* region was never observed. This has to be related to the slight depression in the amplification spectrum occurring in this region, as observed in the spontaneous emission spectra of Fig. 3. The possibility to tune the lasing wavelength is due to two mechanisms. First, remembering that the QWR angle allows adjusting the NOLM low-power transmission, and considering that in continuous-wave regime the intracavity power can be seen as low-power (i.e., much smaller than the NOLM switching power), then in this case the NOLM works as a simple attenuator, whose attenuation can be adjusted between *0* and *0.5* by the QWR.[16] By adjusting in this way the laser intracavity loss, one can modify the balance between absorption and emission that determines the gain spectrum of the EDF,[21] and thus the position of the gain maximum where lasing will take place. Secondly, the residual birefringence present in the cavity and the polarizer are responsible for a coarse filtering effect or wavelength-dependent loss, which can be adjusted through the wave plates and contributes to the selection of the operating wavelength.[22]
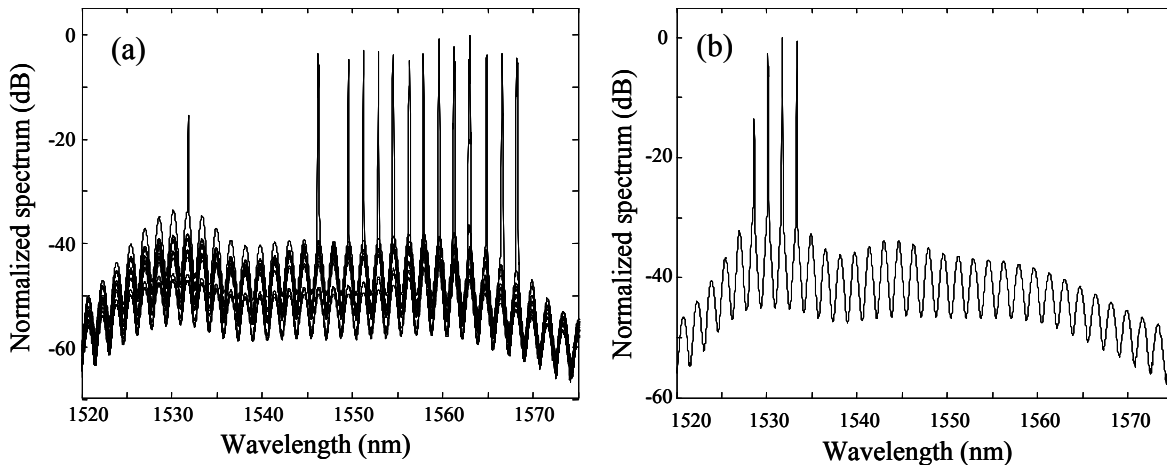
Figure 3. Optical spectra in continuous-wave regime: (a) tunable single-wavelength and (b) four-wavelength operations.

Multiple-wavelength continuous-wave operation was also observed, although in most cases it involved lines with a large wavelength separation between them, whose coexistence is allowed by the homogeneously broadened erbium gain. More interesting and challenging is the observation of simultaneous lasing at closely spaced wavelengths, which are competing for the homogeneously broadened gain. In this study we were able to observe two-, three- and up to four-wavelength operation in the *1530 nm* region, with a wavelength separation of *1.65 nm* in all cases. Fig. 3(b) shows the laser output spectrum in the case of four-wavelength operation. Four-wavelength operation typically remained stable during a few minutes, after which the lower-amplitude line disappeared and the laser operation followed in three-wavelength mode, if no further adjustment was performed. The mechanisms of adjustment of the gain and loss spectra described previously and allowing wavelength tuning are also those that allow adjusting precisely the net gain at different wavelengths, a necessary condition to observe simultaneous lasing of several contiguous lines, in spite of the severe competition between them.[23]

Although self-starting mode locking operation was not observed in this study, for some particular positions of the HWR and QWR, a mechanical stimulation (a kick) results in a sudden widening of the spectrum to a bandwidth of several tens of nm, which indicates the onset of mode locking. The optical signal detected by a 2-GHz photodetector and monitored using a 200-MHz oscilloscope reveals a periodic pulse train whose repetition rate in most cases is *~1.6 MHz* (period = *600 ns*), indicating fundamental frequency mode locking of the ~120-m long laser cavity (Fig. 4(a)).

A closer analysis of the generated pulses reveals their nature of noise-like pulses. Noise-like pulses are large collections of ultrashort pulses with randomly varying amplitudes and durations, which were observed and studied in a number of previous works.[24-32] Fig. 4(b) shows the measured optical autocorrelation of the pulses. It consists of a narrow sub-ps peak riding a wide pedestal that extends beyond the 200-ps measurement window of the autocorrelator. The central spike (*~160 fs*) scales as the average duration of the pulses in the bunch, whereas the pedestal extension (a fraction of a *ns*) is related to the total duration of the noise-like pulse. The duration of the pulse was measured with more precision using a

fast photodetector and a sampling oscilloscope, yielding a value of *~200 ps* at half maximum (Fig. 4(c)). Finally, Fig. 4(d) presents the optical spectra measured at both laser outputs using an optical spectrum analyzer. The very smooth and wide spectrum (*~30 nm* at half maximum) is a common feature of noise-like pulses. Apart from their different left-right asymmetry, which is due to intracavity Raman self-frequency shift, the most noticeable difference between the two spectra is the presence of a ripple due to the filtering element in the spectrum measured at output 2 (which is located just after the filter output), whereas this ripple is not observed at output 1. This tends to demonstrate that, besides causing substantial loss, the periodic filter has little influence on this mode of operation of the laser, as its effect is completely wiped out after one round-trip in the ring section of the laser. In fact, except for the solid curve in Fig. 4(d), the measurements shown in Fig. 4 present no fundamental difference with respect to those obtained from the filterless laser operating in the same mode.[32]
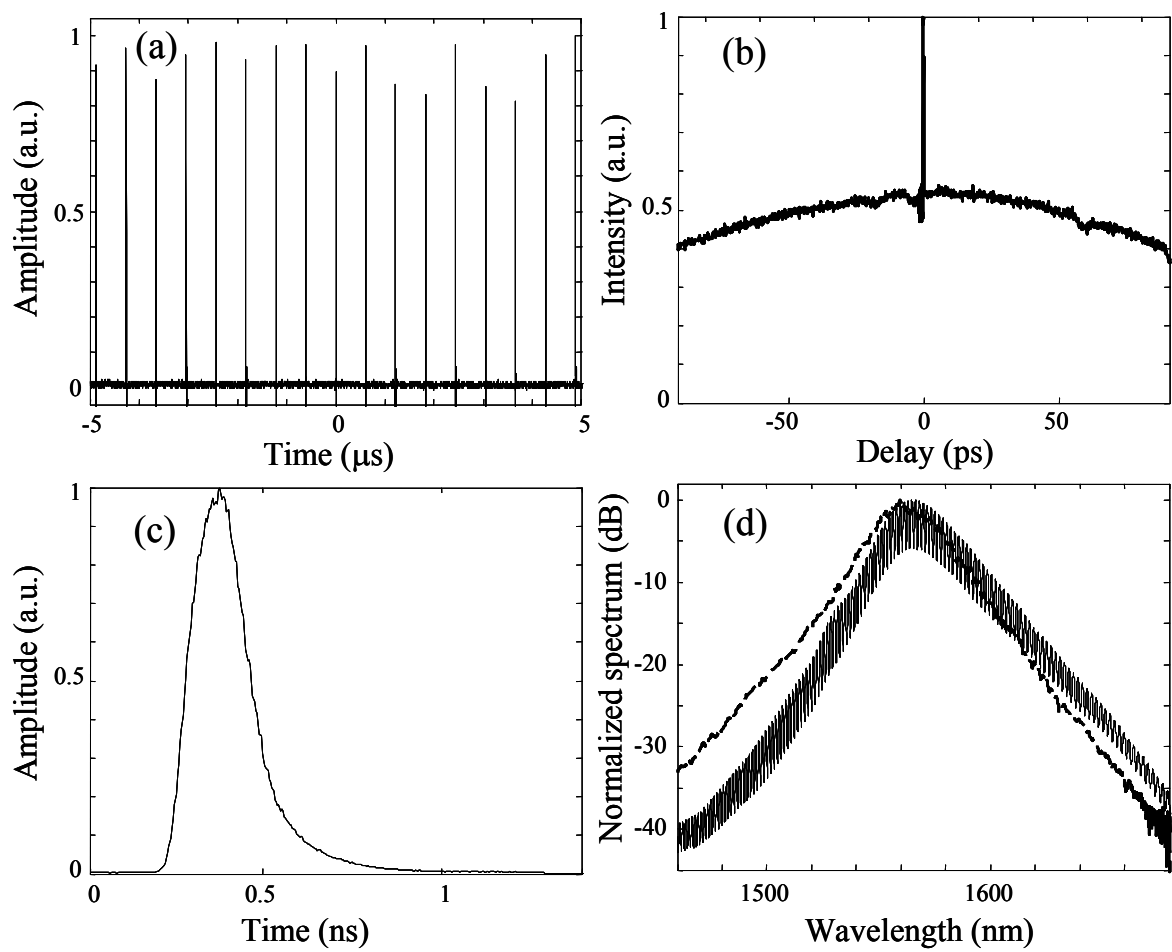
Figure 4. Pulses measured in mode locking regime: (a) pulse train observed with a 2-GHz photodetector and a 200-Mz oscilloscope; (b) optical autocorrelation; (c) single pulse observed with a 25-GHz photodetector and a sampling scope; (d) optical spectrum at output 1 (dashed) and 2 (solid).

A noticeable difference with respect to the filterless case was observed for some adjustments, however, in the form of a second-harmonic mode locking regime. In this case, not one but two noise-like pulses appear in each 600-ns round-trip period (Fig. 5). During most of the time, a stable train of uniformly spaced pulses with a period of *~300 ns* is observed on the scope (Fig. 5(a)), however, typically after a few seconds the second pulse disappears from its central position and reappears immediately close to the first pulse position, then sweeps quickly in time to recover its initial central position where it stabilizes again for a few seconds (Fig. 5(b-d)). This walkoff lasts for a fraction of a second. A different spectral composition between the two pulses propagating in the dispersive cavity could account for this temporal sweeping, however the spectra of the pulses could not be measured individually. The optical spectra measured at outputs 1 and 2 in

this regime are not different from those of Fig. 4(d) for fundamental mode locking, and the autocorrelation trace is similar to that of Fig. 4(b).
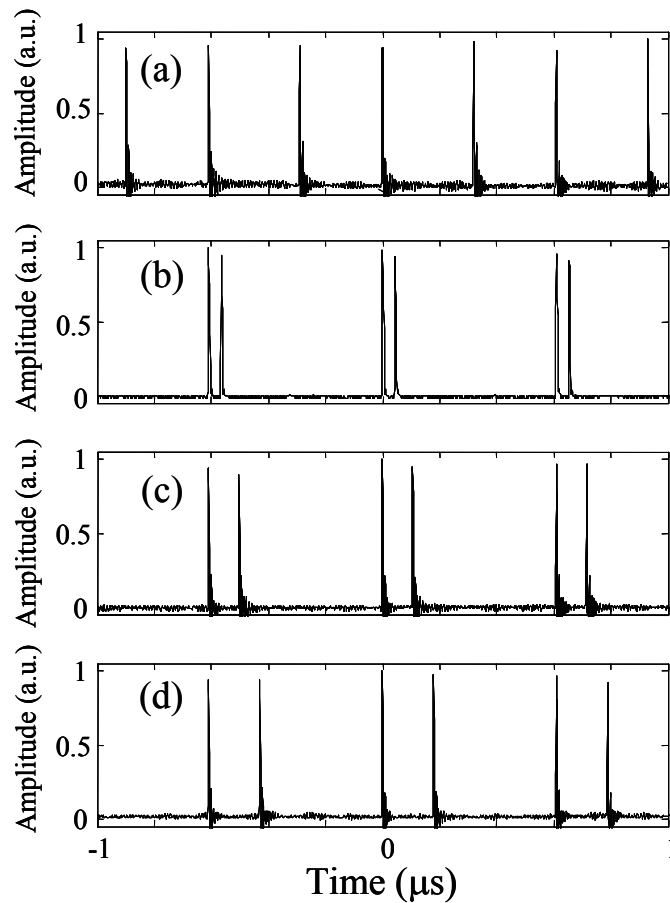
Figure 5. 2nd-harmonic mode-locked pulse train observed with a 2-GHz photodetector and a 200-Mz oscilloscope, at different times.

Finally, a regime of multi-wavelength passive Q-switching was also observed with the figure-eight laser. This regime appears spontaneously for some adjustments of the retarders. In this case, a train of long, highly unstable pulses with duration in the order of *10 μs* is typically generated. As shown in Fig. 6(a), the amplitude, duration and periodicity of these pulses are highly variable. Fig. 6(b) shows the scope trace of the top of a Q-switched pulse, which presents an amplitude modulation in which the cavity fundamental frequency and its 12th harmonic are clearly visible, and which is due to the beat note between resonant cavity modes. The optical spectrum, shown in Fig. 6(c), reveals the multi-wavelength character of the signal. Indeed, it includes a relatively large number of closely spaced spectral components with *1.65 nm* separation. It is noteworthy that their number is typically larger than four, the maximum number of consecutive wavelengths that were observed simultaneously in the continuous-wave regime. One spectral component (at *1556 nm* in Fig. 6(c)) is usually much higher than the others, which is most likely due to the continuous-wave signal accompanying the pulses (see Fig. 6(a)). The 3-dB bandwidth of each line is ~*0.65 nm*, except for the higher one, which is significantly narrower due to the continuous-wave component. This relatively large bandwidth would be compatible with mode locking, however the formation of mode-locked pulses was never observed below the envelope of the Q-switched pulses. Finally, for slightly different adjustments of the wave retarders, the pulses become narrower (duration ~ *1 μs*) and higher, and their occurrence becomes less frequent (Fig. 6(d)).
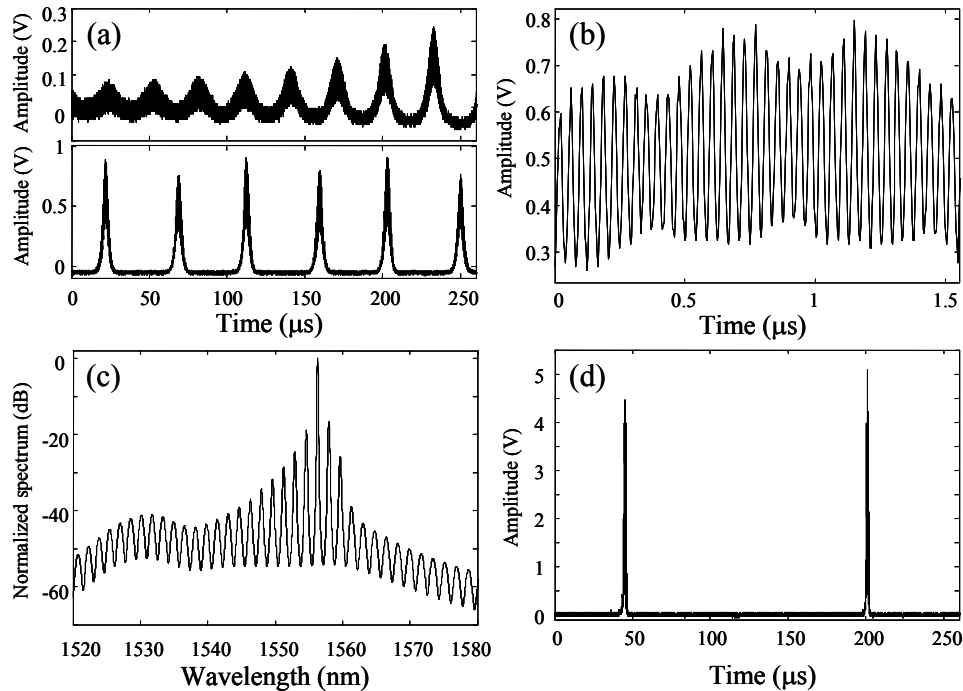
Figure 6. (a) Scope traces of the Q-switched pulse train at different times; (b) detail of a single pulse; (c) optical spectrum; (d) scope trace of irregular giant pulses.

4. NUMERICAL STUDY AND DISCUSSION

The purpose of the numerical study presented here is only to get an insight on the mechanisms that could lead to multiple-wavelength operation in the mode-locked regime of a figure-eight fiber laser, and is not an attempt to reproduce numerically in all their diversity and complexity the experimental results presented above. The scheme under study is similar to the experimental scheme shown in Fig. 1 (with same values of dispersion, nonlinear coefficient, etc), although the NOLM length is substantially shorter (*3 m*) in order to reduce computational time. Moreover, the optical filter is modeled as a double-bandpass filter, so that the multi-wavelength problem is reduced to only two wavelengths for simplicity. The filters are Gaussian, with a wavelength separation $\Delta\lambda$ and 3-dB bandwidth $\delta\lambda$. The gain is assumed to be homogeneously broadened. It is uniform along the EDF and saturates on pulse energy. Numerical simulations are carried out using the nonlinear Schrödinger equations including dispersion, Kerr nonlinearity and gain for the EDF section. The Split-Step Fourier method is used for integration. After a few tens of integration cycles, for properly chosen parameters relatively stable pulses tend to form in regime (although amplitude fluctuations usually remain). Double-wavelength operation is observed in most cases. Note that conventional (i.e., not noise-like) ultrashort pulses are formed, which is to be expected in the case of a short cavity.

Two typical situations are illustrated in Fig. 7, when the wavelength separation is large and small. Dual-wavelength operation is obtained in both cases. In the first case (Fig. 7(a,b)), two pulses coexist, one at each wavelength. Due to fiber dispersion, they are unsynchronized and they present a walkoff that increases after each round-trip. The coexistence of two nearly equal-amplitude pulses can be explained by the filter losses: indeed, a single pulse that would carry the same energy as the two pulses would be higher and shorter, and its spectrum wider, so that it would suffer higher loss through the filter. Two equal-amplitude pulses tend to form because this configuration minimizes the cavity loss (the saturable absorber action of the NOLM has an opposite effect, however it has to be assumed that the filter effect is dominant in this case). In the case of a smaller separation, dual-wavelength operation is again observed, however in this case the walkoff is sufficiently small to be compensated by cross-phase modulation, so that the pulses are synchronized

(Fig. 7(c,d)). The pattern observed in Fig. 7(c) corresponds to the beat note between the two wavelength components. Again, the two wavelength components carry nearly the same energy. In this case, dual-wavelength operation is observed because for the same pulse energy (limited by gain saturation) and duration (limited by filter bandwidth), the amplitude-modulated pattern of Fig. 7(c) has a peak power about two times higher than the single-wavelength pulse (dashed line), and thus suffers lower loss through the NOLM. Again, the loss is minimized when the spectral components have nearly equal amplitudes (corresponding to *100%* modulation of the pulse envelope). In summary, mechanisms involving the filter losses and the nonlinear transmission characteristic of the NOLM tend to favor dual-wavelength mode locking against single-wavelength operation.
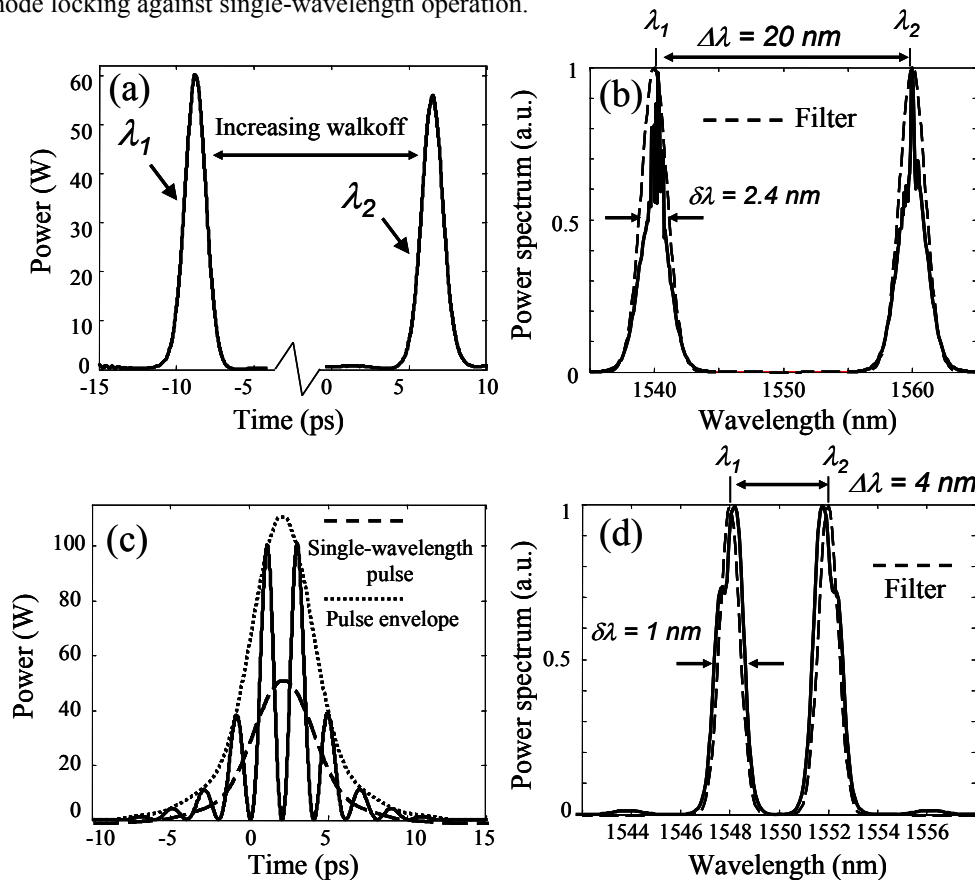
Figure 7. (a,c) Temporal profile and (b,d) optical spectrum of the laser output signal for *Δλ = 20 nm, δλ = 2.4 nm* and for *Δλ = 4 nm, δλ = 1 nm*, respectively.

Although the numerical study presented above is by far simplified, it is still useful to shed some light on the experimental results obtained in section 3 in the pulsed modes. Although the generation of noise-like pulses has been studied in various works,[24-32] no general consensus seems to emerge on the mechanisms involved in their formation. One difficulty is that several proposed mechanisms are able to reproduce the same experimental results (in particular, the double-scaled autocorrelation trace and the wide and smooth optical spectrum). In this context, even more challenging would be to investigate the mechanism of second-harmonic noise-like pulse mode locking that was observed in this work. However, two observations could be helpful: first, considering the wide and smooth spectrum of the noise-like pulses, they suffer high loss through the filter at each round-trip (compare curves of Fig. 4(d)). Secondly, second-harmonic noise-like pulse mode locking was never observed in the filterless laser.[32] This suggests that second-harmonic mode locking could develop as a mechanism to minimize loss through the filter, which could present some similarity with the mechanism described in the numerical study, in the case of asynchronous pulses. The transitory walkoff in the dispersive cavity that was observed experimentally suggests a different spectral composition of the two pulses. However the study is complicated by the large variability of the noise-like pulses: although their global features (total waveform duration, average peak power) remain roughly constant, the details of their inner structure vary widely after successive

round-trips. In particular, the optical spectrum of individual pulses is a very irregular spiky and highly variable pattern, the stable and smooth spectrum that is observed experimentally being obtained only after strong averaging.

Although the physics beyond passive Q-switching is fundamentally different from that of mode locking, the numerical study presented above is still helpful to understand the experimental results in the Q-switching mode. Like passive mode locking, passive Q-switching requires saturable absorber action, however in this case the key action that yields self-pulsing behavior is likely to be due to erbium clusters in the highly doped erbium fiber.[33] In spite of this, the systematic coexistence of a large number of contiguous lines in the Q-switched mode (Fig. 6(c)) can still tentatively be explained considering the NOLM, in the same way as dual-wavelength mode locking in the synchronous case: the beat note between multiple spectral components increases the pulse peak power and thus reduces the loss through the NOLM. The same principle can be evoked to explain the large bandwidth of the lines in each filter window, each of which includes a large number of cavity modes. Although the highest peak power is reached when all these modes are locked in phase together, i.e., when a train of mode-locked ultrashort pulses is formed under the Q-switched pulse envelope, mode locking was never observed, probably because the Q-switched pulse duration (corresponding to *10-15* cavity round-trips) is too short to allow the beat note between modes to evolve into a well formed pulse train starting from spontaneous emission. Finally, another factor may favor the multiwavelength operation in the Q-switching mode: in the case of smooth monochromatic pulses much longer than the time of travel through the NOLM (which is slightly smaller than the round-trip time in the cavity), the signal can be viewed as a continuous-wave signal, and in this case the cross-phase modulation between counter-propagating signals in the loop (which grows with the signal duty cycle) severely alters the NOLM operation,[34] in particular switching power is strongly increased. In contrast, in the case of multiwavelength long pulses, the beat note between the different spectral components reduces the duty cycle, so that cross-phase modulation is more moderate, and the switching power is lower compared to the single-wavelength case. Hence, again multiwavelength operation reduces the loss through the NOLM, by reducing the effect of cross-phase modulation.

5. CONCLUSION

In this work we study numerically and experimentally a novel figure-eight laser scheme including a polarization-imbalanced NOLM with linear input polarization and a periodic filter based on two concatenated fiber tapers. Thanks to the flexibility of the switching characteristic of this NOLM architecture, several modes of operation of the laser were demonstrated experimentally. In the continuous-wave regime, single wavelength operation tunable over more than *20 nm* was demonstrated, as well as simultaneous lasing at up to four contiguous wavelengths with *1.65 nm* separation. Four-wavelength operation was maintained for several minutes without any stabilization mechanism. Non-self-starting mode locking was also observed, in the form of noise-like pulses generation. Both fundamental and second-harmonic mode locking were obtained, with in the latter case a transient walkoff between the two pulses. Finally, an unstable multi-wavelength Q-switching behavior was also demonstrated. A shorter version of the figure-eight laser was simulated numerically, including a double-bandpass filter. The study focused on mode-locked operation. It appeared that dual-wavelength mode-locked operation was obtained in most cases, with the generation of two ultrashort pulses, one at each wavelength, which can be synchronous or asynchronous in the dispersive cavity depending on the wavelength separation. This study suggests that mechanisms involving the filter losses and the nonlinear transmission characteristic of the NOLM contribute to favor dual-wavelength operation with respect to single-wavelength mode locking. Although the numerical study does not reproduce the complexity of the experimental results, it offers some elements to help understanding the processes of second-harmonic noise-like pulse mode locking and even multiwavelength Q-switching that were observed experimentally. We believe that this work will be of interest in the study of multiple-wavelength fiber lasers in both continuous-wave and pulsed regimes, which are attractive for a wide range of applications.

ACKNOWLEDGEMENTS

REFERENCES

[1] Guy, M. J. and Taylor, J. R., "Simultaneous dual polarisation operation of a diode pumped femtosecond fibre laser," Electron. Lett. 29, 2044-2045 (1993).

[2] Noske, D. U., Guy, M. J., Rottwitt, K., Kashyap, R. and Taylor, J. R., "Dual-wavelength operation of a passively mode-locked "figure-of-eight" ytterbium-erbium fibre soliton laser," Opt. Commun. 108, 297-301 (1994).

[3] Zhang, H., Tang, D. Y., Wu, X. and Zhao, L. M., "Multi-wavelength dissipative soliton operation of an erbium-doped fiber laser," Opt. Express 17, 12692-12697 (2009).

[4] Zhao, X., Zheng, Z., Liu, L., Liu, Y., Jiang, Y., Yang, X. and Zhu, J., "Switchable, dual-wavelength passively mode-locked ultrafast fiber laser based on a single-wall carbon nanotube modelocker and intracavity loss tuning," Opt. Express 19, 1168-1173 (2011).

[5] Mao, D., Liu, X. M., Wang, L. R., Li, X. H., Lu, H., Sun, H. B. and Gong, Y. K., "Evolution of dual-wavelength solitons in an erbium-doped fiber laser," Laser Phys. 20, 847-854 (2010).

[6] Luo, A.-P., Luo, Z.-C. and Xu, W.-C., "Switchable dual-wavelength passively mode-locked fiber ring laser using SESAM and cascaded fiber Bragg gratings," Laser Phys. 21, 395-398 (2011).

[7] Luo, A.-P., Luo, Z.-C., Xu, W.-C., Dvoyrin, V. V., Mashinsky, V. M. and Dianov, E. M., "Tunable and switchable dual-wavelength passively mode-locked Bi-doped all fiber ring laser based on nonlinear polarization rotation," Laser Phys. Lett. 8, 601-605 (2011).

[8] Chen, W. C., Luo, Z. C. and Xu, W. C., "The interaction of dual-wavelength solitons in fiber laser," Laser Phys. Lett. 6, 816-820 (2009).

[9] Duling III, I. N., "All-fiber ring soliton laser mode locked with a nonlinear mirror," Opt. Lett. 16, 539–541 (1991).

[10] Doran, N. J. and Wood, D., "Nonlinear optical loop mirror," Opt. Lett. 13, 56-58 (1998).

[11] Fermann, M. E., Haberl, F. and Hofer, M., "Nonlinear amplifying loop mirror," Opt. Lett. 15, 752-754 (1990).

[12] Kuzin, E. A., Korneev, N., Haus, J. W. and Ibarra-Escamilla, B., "Theory of nonlinear loop mirrors with twisted low-birefringence fiber," J. Opt. Soc. Am. B 18, 919–925 (2001).

[13] Kuzin, E. A., Ibarra-Escamilla, B., Garcia-Gomez, D. E. and Haus, J. W., "Fiber laser mode locked by a Sagnac interferometer with nonlinear polarization rotation," Opt. Lett. 26, 1559-1561 (2001).

[14] Ibarra-Escamilla, B., Pottiez, O., Kuzin, E. A., Haus, J. W., Grajales-Coutiño, R. and Zaca-Moran, P., "Experimental investigation of self-starting operation in a F8L based on a symmetrical NOLM," Opt. Commun. 281, 1226-1232 (2008).

[15] Ibarra-Escamilla, B., Pottiez, O., Haus, J. W., Kuzin, E. A., Bello-Jimenez, M. and Flores-Rosas, A., "Wavelength-tunable picosecond pulses from a passively mode-locked figure-eight Erbium-doped fiber laser with a Sagnac fiber filter," J. European Opt. Soc. 3, 08036-1-4 (2008).

[16] Pottiez, O., Kuzin, E.A., Ibarra-Escamilla, B. and Mendez-Martinez, F., "Theoretical investigation of the NOLM with highly twisted fibre and a $\lambda/4$ birefringence bias," Opt. Commun. 254, 152-167 (2005).

[17] Ibarra-Escamilla, B., Kuzin, E. A., Zaca-Moran, P., Grajales-Coutiño, R., Mendez-Martinez, F., Pottiez, O., Rojas-Laguna, R. and Haus, J.W., "Experimental investigation of the nonlinear optical loop mirror with twisted fiber and birefringence bias," Opt. Express 13, 10760-10767 (2005).

[18] Monzon-Hernandez, D., Martinez-Rios, A., Torres-Gomez, I. and Salceda-Delgado, G., "Compact optical fiber curvature sensor based on concatenating two tapers," Opt. Lett. 36, 4380-4382 (2011).

[19] Tanemura, T. and Kikuchi, K., "Circular birefringence fiber for nonlinear optical signal processing," J. Lightwave Technol. 24, 4108-4119 (2006).

[20] Pottiez, O., Ibarra-Escamilla, B. and Kuzin, E.A., "Large signal-to-noise-ratio enhancement of ultrashort pulsed optical signals using a power-symmetric Nonlinear Optical Loop Mirror with output polarization selection," Opt. Fiber Technol. 15, 172-180 (2009).

[21] Franco, P., Midrio, M., Tozzato, A., Romagnoli, M. and Fontana, F., "Characterization and optimization criteria for filterless erbium-doped fiber lasers," J. Opt. Soc. Am. B 11, 1090–1097 (1994).

[22] Gonzalez-Garcia, A., Pottiez, O., Ibarra-Escamilla, B. and Kuzin, E. A., "Switchable and tuneable multi-wavelength Er-doped fibre ring laser using Sagnac filters," Laser Physics 20, 720-725 (2010).

[23] Alvarez-Tamayo, R. I., Duran-Sanchez, M., Pottiez, O., Kuzin, E. A., Ibarra-Escamilla, B. and Flores-Rosas, A., "Theoretical and experimental analysis of tunable Sagnac high-birefringence loop filter for dual-wavelength laser application," Applied Optics 50, 253-260 (2011).

[24] Horowitz, M., Barad, Y. and Silberberg, Y., "Noiselike pulses with a broadband spectrum generated from an erbium-doped fiber laser," Opt. Lett. 22, 799–801 (1997).

[25] Horowitz, M. and Silberberg, Y., "Control of noiselike pulse generation in erbium-doped fiber lasers," IEEE Photon. Technol. Lett. 10, 1389-1391 (1998).

[26] Kang, J. U., "Broadband quasi-stationary pulses in mode-locked fiber ring laser," Opt. Commun. 182, 433-436 (2000).

[27] Takushima, Y., Yasunaka, K., Ozeki, Y. and Kikuchi, K., "87 nm bandwidth noise-like pulse generation from erbium-doped fibre laser," Electron. Lett. 41, 399-400 (2005).

[28] Tang, D. Y., Zhao, L. M. and Zhao, B., "Soliton collapse and bunched noise-like pulse generation in a passively mode-locked fiber ring laser," Opt. Express 13, 2289-2294 (2005).

[29] Zhao, L. M. and Tang, D. Y., "Generation of 15-nJ bunched noise-like pulses with 93-nm bandwidth in an erbium doped fiber ring laser," Appl. Phys. B 83, 553-557 (2006).

[30] Zhao, L. M., Tang, D. Y. and Wu, J., "Noise-like pulse in a gain-guided soliton fiber laser," Opt. Express 15, 2145-2150 (2007).

[31] Kobtsev, S., Kukarin, S., Smirnov, S., Turitsyn, S. and Latkin, A., "Generation of double-scale femto/pico-second optical lumps in mode-locked fiber lasers," Opt. Express 17, 20707-20713 (2009).

[32] Pottiez, O., Grajales-Coutiño, R., Ibarra Escamilla, B., Kuzin, E. A. and Hernandez-Garcia, J. C., "Adjustable noise-like pulses from a figure-eight fiber laser," Applied Optics 50, E24-E31 (2011).

[33] Colin, S., Contesse, E., Le Boudec, P., Stephan, G. and Sanchez, F., "Evidence of a saturable-absorption effect in heavily erbium-doped fibers," Opt. Lett. 21, 1987-1989 (1996).

[34] Pitois, S., "Influence of cross-phase modulation in SPM-based nonlinear optical loop mirror," Opt. Commun. 253, 332-337 (2005).